INSIGHTS INTO THE OXIDATION MECHANISM OF MOLYBDENUM IN MOLTEN GLASS

INE VANMOORTEL, JOOST DE STRYCKER*, EDUARD TEMMERMAN, ANNEMIE ADRIAENS

Department of Analytical Chemistry, Ghent University, Krijgslaan 281-S12, B-9000 Ghent, Belgium
**Arcelor Innovation - R&D, OCAS N.V., J. Kennedylaan 3, B-9060 Zelzate, Belgium*

E-mail: annemie.adriaens@ugent.be

Submitted July 13, 2007; accepted November 30, 2007

Keywords: Oxidation, Mechanism, Glass melts, Molybdenum

This study focuses on the elaboration of the oxidation mechanism of molybdenum in a molten glass. More specifically it was sought to examine whether the anodic dissolution of molybdenum occurs in one or more steps and what the reaction products are. The work was performed in two steps. First the reaction of molybdenum ions in a glass melt at a platinum electrode was investigated. This was followed by the study of the corrosion reactions at a molybdenum electrode in this molten glass. Experiments showed that the oxidation of metallic molybdenum occurs in three steps: $Mo \rightarrow Mo^{3+}(glass) + 3e^-$ *(I);* $Mo^{3+}(glass) \rightarrow \rightarrow Mo^{4+}(surface/glass) + e^-$ *or* $Mo \rightarrow Mo^{4+}(surface/glass) + 4e^-$ *(II);* $Mo^{4+}(surface/glass) \rightarrow Mo^{6+}(glass) + 2e^-$ *or* $Mo \rightarrow \rightarrow Mo^{6+}(glass) + 6e^-$ *(III).*

INTRODUCTION

The electric melting of glass is a technique with increasing importance in the glass and enamel production industry as a result of various technical and ecological advantages [1]. The procedure involves bringing heat into the glass melt by means of the Joule effect using an ac current through electrodes immersed in the melt.

Today, molybdenum is commonly used as electrode material for glass melting. It has a high melting point, a high thermal and electrical conductivity and it is mechanically stable up to temperatures of 1600°C. The most important problem, however, associated with the electrical glass melting and the use of molybdenum electrodes is the significant corrosion of the electrode material. This corrosion process considerably limits the life of the electrodes, at the same time leading to the pollution of the glass/enamel.

Several studies on the corrosion behaviour of molybdenum electrodes in glass melts have been published [2-16]. They involve studies of the corrosion reaction including the influence of different process parameters and studies concerning the corrosion protection. Only a few studies also treat the corrosion mechanism, many of them in lead-containing glasses [2-3, 9-10, 13]. All of them indicate the occurrence of several steps in the oxidation reaction of molybdenum with Mo (VI) as final reaction product. However, the path followed and the intermediate products formed vary according to the study undertaken.

This study focuses on the elaboration of the oxidation mechanism of molybdenum in a molten glass. The aim was to examine whether the anodic dissolution of molybdenum occurs in one or more steps, and what the reaction products are. The elucidation of the corrosion mechanism is not only important from a fundamental point of view but is also crucial for obtaining a better insight into the problems which arise in industrial ovens.

The paper discusses first the reaction of molybdenum ions in a glass melt with simplified composition at a platinum electrode. In a second step the corrosion reactions at a molybdenum electrode in this molten glass have been investigated. Techniques used include cyclic voltammetry (CV) and square wave voltammetry (SWV). The data are backed up using results from scanning electron microscopy with energy dispersive X-ray analysis (SEM-EDX), X-ray photoelectron spectroscopy (XPS) and X-ray diffraction (XRD).

EXPERIMENTAL

A vertical tube furnace was modified to be powered with dc current in order to avoid the effect of an ac current on the electrochemical experiments, as previously described by Rüssel et al. [17-18]. A water cooled flange of stainless steel was placed on top of the furnace. In this flange the reference and counter electrode are attached.

The reference electrode is a rod of yttria stabilised zirconia, the upper part of which is cemented into an alumina tube with a ceramic mortar. Inside this tube a pressure contact with the zirconia is made with the aid of a platinum wire and as reference gas air is blown through the tube [19]. All potentials mentioned in this paper refer to this reference. The counter electrode is a platinum plate with a surface area of approximately 3 cm^2. The working electrode is an inlaid disc electrode. For the study of the reactions of molybdenum ions a platinum electrode is used, whereas for the study of the corrosion reaction(s) of metallic molybdenum a molybdenum electrode is employed. These inlaid disc electrodes are constructed according to the procedure developed by De Strycker et al. [20]: a platinum rod (3 mm diameter; 99.95 % pure) respectively a molybdenum rod (5 mm diameter; 99.98 % pure) is fixed in an alumina tube (8 mm inner diameter; 99.7 % pure) with a ceramic binder in such a way that only the cross section of the rod is used as electrode surface. Contact is made with a platinum wire. The alumina tube was purged with pure nitrogen to avoid contact of the molybdenum with air.

A fresh surface of the working electrode is obtained by polishing with SiC-emery paper, type 1200 grit for 30 s. To smoothen this relatively rough surface it was further polished on a polishing cloth with alumina powder of successively 1.0 and 0.05 μm particle size for 5 and 10 min respectively. The polishing sequence was carried out on a disk polishing machine. To remove any adsorbed alumina particles an ultrasonic cleaning step was introduced.

The electrochemical cell, an alumina crucible, was filled with the melt and was lifted into the furnace with the aid of an alumina tube placed on two lab jacks. This system allows one to control the position in the furnace very precisely. Checking of the contact between electrodes and the melt was carried out through electrical conductivity measurements. After dipping in the reference and counter electrode the furnace was flushed with pure nitrogen and the working electrode was immersed and attached in the water cooled flange. Subsequently the atmosphere was changed by blowing air into the furnace. The operating temperature for all tests was 1473 K.

The choice of the glass melt was based on a prelimiary study in which 50 commercial melts were compared for their chemical composition. The criteria of the melt used in this work included having a representative, but also a relative simple glass which did not contain any electrochemically active substances. Its chemical composition, both theoretically (i.e. the aimed composition) as well as the actual one is given in Table 1. For the first set of experiments, this composition was modified by the addition of 2.5% MoO_3. All reagents used to prepare the melts were of analytical grade.

For all electrochemical experiments a PC controlled potentiostat and software package type GPES 4.5 (Autolab PGSTAT20 from ECO Chemie) was used. SEM-EDX analyses were performed on a Philips 505 with 30 kV acceleration voltage. XRD data were obtained with a Siemens D5000 theta-2theta diffractometer using a copper anode (λ = 1.5406 Å). Signals were acquired between 2θ values 5° and 90°. The XPS measurements were recorded with a Perkin-Elmer Phi ESCA 5500 system equipped with a monochromated 450 W Al K source. Experiments were recorded with 220 W source power and an angular acceptance of ±7°. The analyser axis made an angle of 45° with the specimen surface. Wide scan spectra were measured over a binding energy range of 0-1000 eV and a pass energy of 187.85 eV. The Mo 3d core levels were recorded with a step of 0.05 eV and a pass energy of 11.75 eV.

Table 1. Chemical composition of the basic glass melt.

Oxide	Theoretical (wt.%)	Actual (wt.%)
SiO_2	64.0	62.8 ± 0.3
Na_2O	18.0	18.2 ± 0.2
CaO	8.0	7.8 ± 0.1
B_2O_3	5.0	4.9 ± 0.1
MgO	3.0	3.5 ± 0.1
Al_2O_3	1.0	1.8 ± 0.1
K_2O	1.0	0.8 ± 0.1
Fe_2O_3		0.12 ± 0.01
ZrO_2		0.08 ± 0.01

RESULTS AND DISCUSSION

Voltammetric behaviour of molybdenum ions

Figure 1 shows a set of cyclic voltammetric curves of the glass melt (top) and the glass melt containing 2.5 wt.% MoO_3 (bottom). The voltammograms were recorded at 1473 K using a platinum electrode and this for different potential regions. All measurements started at 0.1 V versus the reference electrode (RE). At this potential it can be assumed that the main form of molybdenum in the melt is Mo (VI) [2-3, 9-10, 13]. The vertex potentials varied from -0.80 to -1.15 V vs. RE. In each potential region one or more anodic and cathodic reactions, indicated with the letters a to f, can be observed. On the basis of the occurrence of the anodic and cathodic waves as a function of the vertex potentials, it can be assumed that the cathodic and anodic wave, indicated respectively as a and f in Figure 1, are caused by reactions of the same redox couple. The same hypothesis can be made for cathodic wave b and anodic peak d and for the additional increase in the cathodic current (region c in Figure 1) at potentials more negative than -1.05 V vs. RE and the corresponding anodic peak e. As a result a stepwise reduction (and re-oxidation) of Mo(VI) ions can be assumed.

In order to verify these assumptions, stripping voltammetric experiments were performed. The enrichment step was performed by applying a negative potential situated in a reduction plateau and was then followed by an anodic polarisation. Figure 2a shows the cyclic voltammograms acquired after the platinum working electrode was held at -0.85 V vs. RE, a potential situated in the first reduction plateau (a in Figure 1), for respectively 20, 40 and 60 seconds. A longer enrichment time clearly leads to an increase in the anodic peaks situated around -0.55 V (d in Figure 1). Figure 2b shows the cyclic voltammograms acquired after the platinum working electrode was held at 1.00 V vs. RE, a potential situated in the second reduction wave (b in Figure 1), for respectively 20, 40 and 60 seconds. Also here an increase in the anodic current is seen, more specifically for the anodic peak d (Figure 1), with longer enrichment times. Also the relationship between de cathodic wave (b) and the anodic wave (d) is confirmed. It can also be seen that reaction (e) is superimposed as a shoulder on the anodic wave (d).

Additional square wave voltammetric experiments were performed to facilitate the identification of the redox reactions. Literature data show that this technique has an excellent sensitivity and high resolution for measurements in glass melts [17, 21-23]. Figure 3 presents two square wave voltammetric curves: one of the basic glass melt and one of the same glass melt containing 2.5 wt.% MoO_3. Both curves were recorded at a platinum electrode at a temperature of 1473 K using a frequency of 10 Hz. At least three peaks can be observed in the voltammetric curve of the glass melt containing 2.5 wt.% MoO_3: the E_p values are at -0.38 V, -0.78 V vs. RE and -0.95 V vs. RE. At the anodic side of the second peak ($E_p \cong -0.78$ V vs. RE) a shoulder can be observed. Comparison of this voltammogram with that recorded in the basic glass melt under the same experimental conditions reveals that the first peak, $E_p \cong -0.38$ V vs. RE, cannot be attributed to a reaction of the molybdenum ions as this peak is also present in the basic smelt. The others peaks apparently are caused by reduction reactions of molybdenum ions.

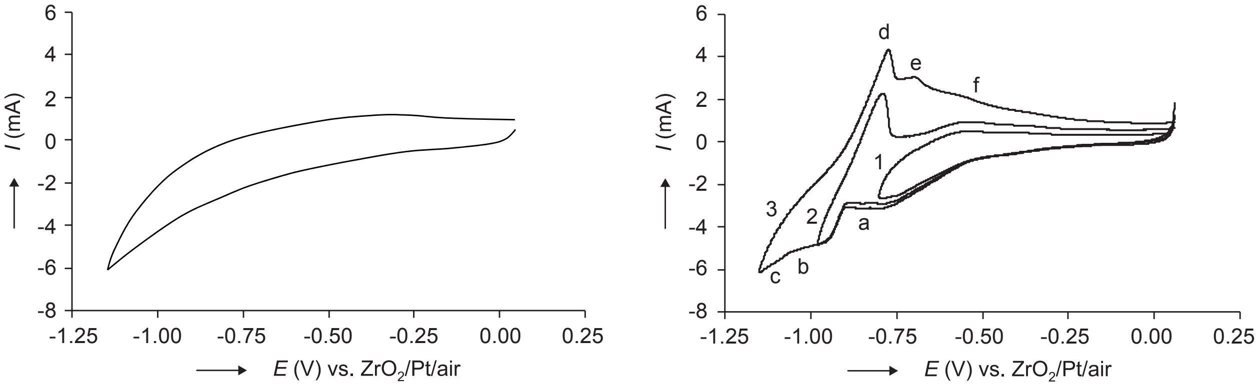

a) b)

Figure 1. Cyclic voltammograms acquired in the basic glass melt (top) and the basic including 2.5 wt.% MoO_3 (bottom) at 1473 K. Scan rate = 100 mV/s; E_{start} = 0.1 V; vertex potentials -0.80 (1), -0.98 (2) and -1.15 V (3).

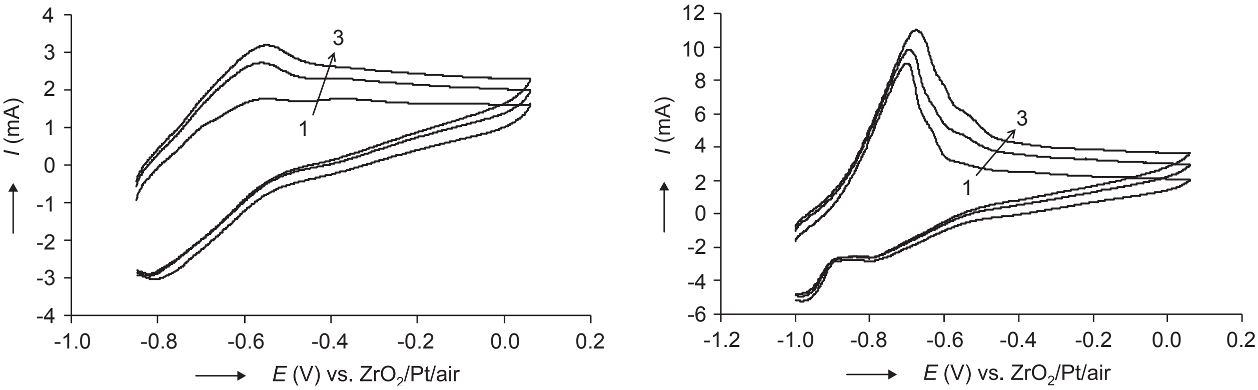

a) b)

Figure 2. Cyclic voltammograms acquired in the basic glass melt including 2.5 wt.% MoO_3 at 1473 K after a cathodic polarisation at -0.85 V (a) and -1.00 V (b). The numbers indicate different enrichment times: (1) 20 seconds, (2) 40 seconds and (3) 60 seconds. Scan rate = 100 mV/s; vertex potential = 0.10 V.

As a final experiment in this series, potential step experiments immediately followed by SEM-EDX analyses of the working electrode were performed. A platinum plate was used as a working electrode. Two surface conditions were examined. A potential of -0.895 V vs. RE, situated in the first reduction plateau (a in Figure 1) was applied to 'electrode 1' for 1800 s. 'Electrode 2' was held for 2700 s at -1.085 V vs RE, which corresponds with the second reduction wave (b in Figure 1). After the polarisation, the electrodes were pulled from the glass melt and rapidly cooled to room temperature in air. The adhering glass was removed mechanically. Surface analysis of the electrode surfaces by SEM-EDX shows evidence for molybdenum deposition on both electrodes. The latter is demonstrated in Figure 4. Even though the molybdenum peaks are rather weak, they indicate the electrochemical reaction of molybdenum ions at the two potential values. In order to obtain information about the oxidation state of this molybdenum deposition, the electrode surfaces were investigated using XPS and XRD. Figure 5 shows the XPS data of electrode 1, which clearly demonstrates the presence of molybdenum next to platinum. Comparing the molybdenum with reference spectra, it could be concluded that molybdenum is present in metallic form. XRD data of electrode 2 are shown in Figure 6. Almost all peaks can be attributed to one of the three phases: platinum, a platinum molybdenum phase (Pt_3Mo) and molybdenum trioxide (MoO_3).

While cyclic voltammograms point towards a two-step reduction, square wave data seem to indicate three reduction steps. If the latter data are caused by the same reduction reactions of molybdenum ions as those detected in the cyclic voltammograms, the square wave peak potentials must equal the half wave potentials of the corresponding cyclic voltammogram. Table 2 summarizes these data and shows a clear agreement for the last peak. The other data, however, do not match. The half wave potential of the voltammetric peak a (Figure 1) does not equal the square wave voltammetry peak potential of peak 2 (Figure 3), nor the one of the anodic shoulder (Figure 3, 2s), but is rather situated in between. Considering the better resolution of the square wave technique, this discrepancy can easily be explained. The first reduction wave in the cyclic voltammetric curve is caused by two overlapping successive reaction steps but

Table 2. Square wave voltammetric peak and cyclic voltammetric half wave potentials observed for the glass melt containing 2.5 wt.% MoO_3.

SQW, f = 10 Hz E_p (V) vs. RE	CV, v = 0.1 V/s $E_{1/2}$ (V) vs. RE
-0.628 (Figure 3, peak 2s)	–
-0.769 (Figure 3, peak 2)	-0.695 (Figure 1, peak a)
-0.921 (Figure 3, peak 3)	-0.926 (Figure 1, peak b)

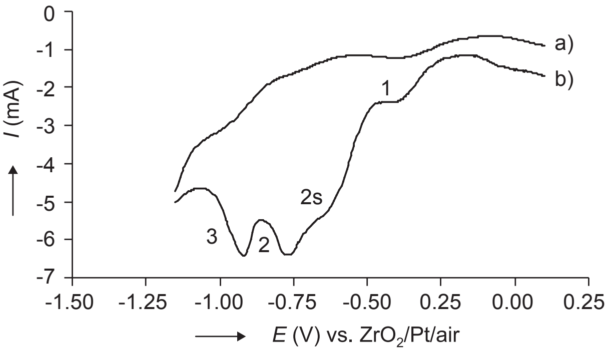

Figure 3. Square wave voltammetric curve of the basic glass melt (a) and of the same glass melt containing 2.5 wt.% MoO_3 (b). Both curves were recorded at a platinum electrode at a temperature of 1473 K and a frequency of 10 Hz.

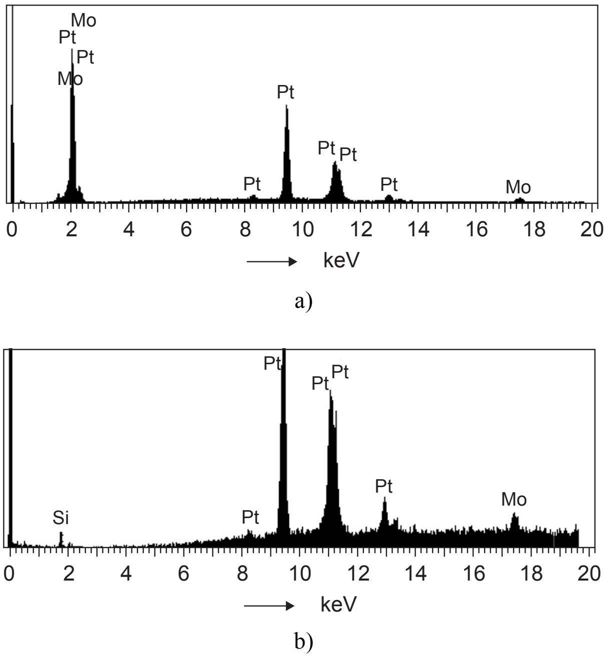

a)

b)

Figure 4. SEM-EDX spectra (30 keV, 20 mA, 100 s) of the platinum electrode surface after polarisation during 1800 s at a potential of -0.895 V (a) and -1.085 V (b) in a glass melt containing 2.5 wt.% MoO_3 at 1473 K.

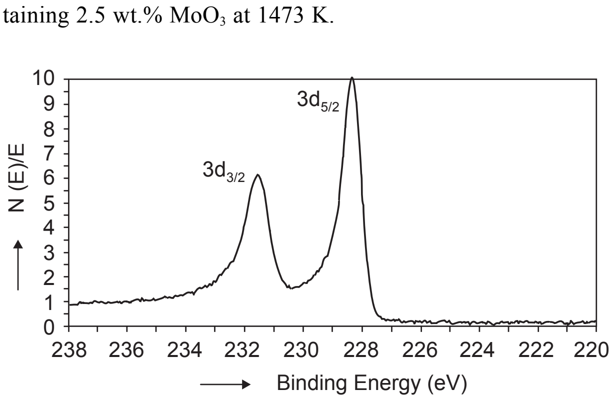

Figure 5. Molybdenum XPS spectrum of the platinum electrode surface after polarisation during 1800 s at a potential of -0.895 V in a glass melt containing 2.5 wt.% MoO_3 at 1473 K.

the characteristic potentials for these reactions are too close to each other to be distinguished. With the aid of square wave voltammetry two reactions can be detected but the peaks are still not fully separated.

Although the characteristic potentials for the first and second step are too close to each other to be analysed separately, a general mechanism can be proposed taking into account the surface analysis data. The electrochemical experiments were started at 0.1 V versus RE and at this potential it can be assumed that the oxidation state of the molybdenum is +VI. In addition the XPS data of electrode 1 show that the final product of the two successive reduction reactions is metallic molybdenum. As a result, the following reaction mechanism can be suggested:

$$Mo^{6+} + xe^{-} \rightarrow Mo^{(6-x)+} \tag{4}$$

$$Mo^{(6-x)+} + \left(6-x\right)e^{-} \rightarrow Mo^{0} \tag{5}$$

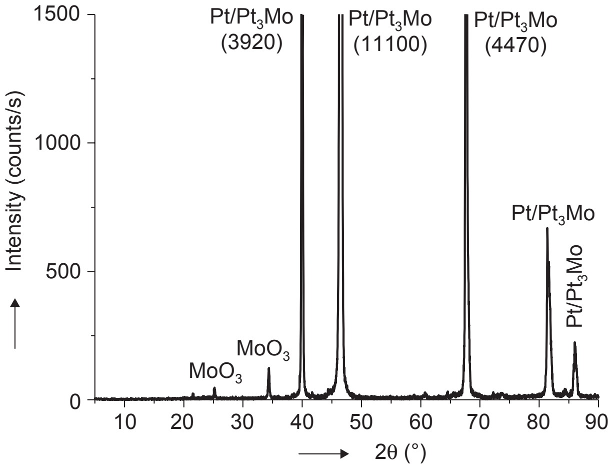

Figure 6. XRD pattern of the surface of a platinum electrode after polarisation during 2700 s at a potential of -1.085 V in a glass melt containing 2.5 wt.% MoO_3 at 1473 K. Peak maximum of Mo between parentheses.

In literature the observed reduction and oxidation reactions of the molybdenum system at a platinum electrode in a soda-lime silicate melt are assumed to originate from the Mo(VI)/Mo(III) and Mo(III)/Mo(0) couples [3]. However, in this investigation no experimental evidence could be found for the Mo (III) as reaction product of the first reduction step.

XRD analyses of the separate glass samples (not shown here) proved that the layer consists of metallic molybdenum and elementary silicon, while no evidence could be found for the formation of MoSix. Therefore, it can be assumed that the last reduction peak (Figure 1, peak b or Figure 3, peak 2) is related to the reduction of silicon ions to elementary silicon:

$$SiO_2 + 4e^{-} \rightarrow Si^{0} + 2O^{2-} \tag{6}$$

In comparison with the reduction of silicon ions at a pure platinum electrode, the reaction at the 'modified' electrode takes place at more positive potentials. The latter explains the fact that this reduction wave only can be observed in the glass containing MoO_3.

Anodic behaviour of metallic molybdenum

In the second part of this study the oxidation behaviour of metallic molybdenum was investigated. Two curves acquired during two identical, but independent experiments are presented in Figure 7. Comparison of the two curves shows that the shape and the position of the anodic peaks are reproducible: in both cases three anodic peaks can be distinguished, which indicates a three-step oxidation of metallic molybdenum. On the other hand the current intensity is not reproducible, which can most probably be explained by the reactive, not reproducible electrode surface. The latter implies that on the basis of these experiments only qualitative information about the corrosion reaction can be obtained.

The most important problem associated with the interpretation of the data, however, is the fact that the three anodic peaks are not fully separated. As a result, the identification of the reaction steps on basis of the electrochemical data becomes very difficult, if not impossible. Therefore a combination of potential step experiments with surface analysis was performed. In this experiment three molybdenum electrodes were polarised for 3600 s at the different oxidation peak potentials. Afterwards they were cooled to room temperature rapidly. Another sample was prepared under open circuit potential conditions. This served as reference sample. In the XRD spectrum (Figure 8a) of the non-polarised molybdenum electrode only characteristic peaks of metallic molybdenum were detected. The peaks in the spectra of the polarised electrodes (Figure 8b) can be attributed to two phases: MoO_2 and metallic Mo. The only difference is the intensity of the MoO_2 peaks (not shown). The most intensive MoO_2 peaks are detected at the surface of the molybdenum electrode polarised at the second oxidation peak ($E_p \simeq$ -0.60 vs. RE), the spectrum of the electrode polarised at the first oxidation peak ($E_p \cong$ -0.73 vs. RE) showed the least intensive peaks.

In order to identify the other reaction steps, changes in the colour of the glass melt used during the polarisation were studied. The colour of a glass can be an indication for the oxidation state of some polyvalent ions in the melt. The primary glass used in this study contains neither electroactive nor colouring substances. If during the polarisation of the molybdenum electrodes colour changes take places, they can only be caused by corrosion products of the molybdenum. The polarisation at the first oxidation peak gives rise to a dark green colour, which according to literature correlates with the colour of Mo(III) [2]. The latter implies that the formation of Mo^{3+} as an intermediate during the oxidation process is the most likely step. This hypothesis is confirmed in literature by Rüssel et al. [2, 4]. Polarisation of the molybdenum at the second oxidation peak potential leads to a much paler colour in the melt, which can be explained by some remaining Mo^{3+} or a small amount of dissolved Mo^{4+}. The polarisation at the last peak potential causes no colouration, which is in agreement with Mo^{6+} as the final product of the corrosion process.

A combination of the results described above allows us to propose a reaction mechanism for the corrosion process of molybdenum in the molten glass.

$$Mo \rightarrow Mo^{3+}(glass) + 3e^{-} \tag{7}$$

$$\begin{gathered} Mo^{3+}(glass) \rightarrow Mo^{4+}(surface/glass) + e^{-} \\ \text{or} \quad Mo \rightarrow Mo^{4+}(surface/glass) + 4e^{-} \end{gathered} \tag{8}$$

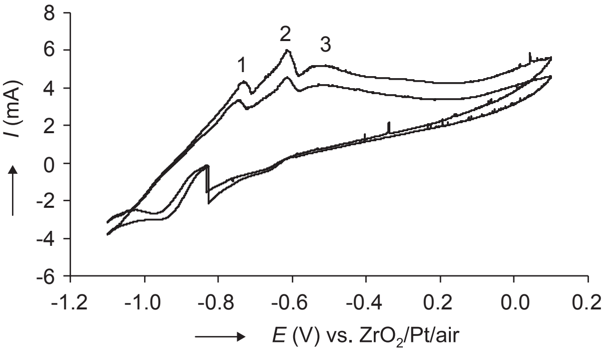

Figure 7. Cyclic voltammograms recorded at a molybdenum electrode in a glass melt at 1473 K. Scan rate = 1 mV/s; E_{start} = = OCP; vertex potentials = -1.15 and 0.1 V.

$$\begin{gathered} Mo^{4+}(surface/glass) \rightarrow Mo^{6+}(glass) + 2e^{-} \\ \text{or} \quad Mo \rightarrow Mo^{6+}(glass) + 6e^{-} \end{gathered} \tag{9}$$

CONCLUSIONS

In this study, experiments were conducted to investigate the corrosion mechanism of molybdenum. On the one hand cyclic and square wave voltammograms were recorded at a platinum electrode in the basic glass melt modified with molybdenum oxide additions. On the other hand cyclic voltammetric experiments at a molybdenum electrode were performed. As a result of these experiments a stepwise reduction of Mo(VI) ions as well as a stepwise oxidation of metallic molybdenum was revealed. In both cases, several, not fully separated waves or peaks attributed to reactions of molybdenum or its ions were detected. The characteristic potentials for the successive reaction steps are relatively close to each other when the peak broadening, as a result of the temperature required for measuring in molten glass is taken into account. As a result, the identification of the reaction steps on basis of the electrochemical data was not possible, but a combination with surface analysis techniques and visual changes in the glass melt allowed to formulate the following mechanism:

$$Mo \rightarrow Mo^{3+}(glass) + 3e^{-} \tag{10}$$

$$\begin{gathered} Mo^{3+}(glass) \rightarrow Mo^{4+}(surface/glass) + e^{-} \\ \text{or} \quad Mo \rightarrow Mo^{4+}(surface/glass) + 4e^{-} \end{gathered} \tag{11}$$

$$\begin{gathered} Mo^{4+}(surface/glass) \rightarrow Mo^{6+}(glass) + 2e^{-} \\ \text{or} \quad Mo \rightarrow Mo^{6+}(glass) + 6e^{-} \end{gathered} \tag{12}$$

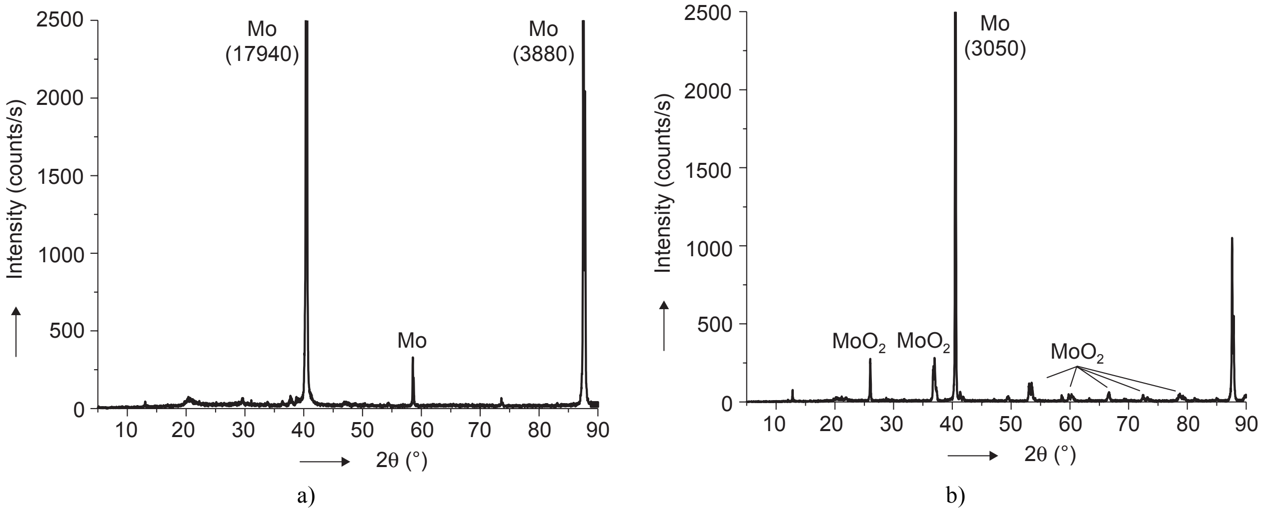

a) b)

Figure 8. XRD patterns of the surface of a molybdenum electrode (a) after being held at the open circuit potential during 3600 s in the basic glass melt at 1473 K and (b) after being polarized at -1.085 V during 3600 s in the basic glass melt at 1473 K. Peak maxima between parentheses.

Acknowledgement

The authors acknowledge the help of O. Janssens and U. Demeter at the Department of Solid State Sciences (Ghent University) for performing the surface analyses.

References

1. Staněk J.: *Electric Melting of Glass*, Elsevier, Amsterdam 1977.
2. Rudolph T., Balazs G. B., Rüssel C., Tomandl G.: Glastech.Ber. *61*, 177 (1988).
3. Balazs G. B., Rüssel C.: J.Non-Cryst.Solids *105*, 1 (1988).
4. Matěj J.: Glastech.Ber. *61*, 1 (1988).
5. Matěj J.: Glastech.Ber. *63*, 8 (1990).
6. Holzwarth S., Rüssel C., Tomandl G.: Glastech.Ber. *64*, 195 (1991).
7. Rüssel C.: Glastech.Ber. *64*, 123 (1991).
8. Matěj J., Bernard V.: Glastech.Ber. *66*, 1 (1993).
9. Matěj J., Freivolt Š., Hulínský V.: Ceramics-Silikáty *40*, 1 (1996).
10. Sundaram S., Speyer R. F.: J.Am.Ceram.Soc. *79*, 1851 (1996).
11. Matěj J., Krupková E., Mamo K.: Ceramics-Silikáty *42*, 132 (1998).
12. Rüssel C., Kampfer A.: Glass Science Technology: Glastech.Ber. *71*, 6 (1998).
13. Matěj J., Krupková E., Hulínský V.: Ceramics-Silikáty *46*, 133 (2002).
14. Matěj J., Kocourová R., Langrová A., Čierna V: Ceramics-Silikáty *47*, 162 (2003).
15. Černa V., Matěj J., Maryška M., Hulínský V., Langrová A.: Ceramics-Silikáty *50*, 32 (2006).
16. Vanmoortel I., De Strycker J., Temmerman E., Adriaens A.: J.Non-Cryst.Solids *353*, 2179 (2007).
17. Freude E., Rüssel C.: Glastech.Ber. *60*, 202 (1987).
18. Rüssel C., Sprachmann G., J.Non-Cryst.Solids *127*, 197 (1991).
19. Ruz P., Lenhart A., Schaeffer H. A.: Fortschr.Deutsch. Keram.Ges. *1*, 138 (1985).
20. De Strycker J., Westbroek P., Temmerman E.: J.Non-Cryst.Solids *289*, 106 (2001).
21. Montel C., Rüssel C., Freude E.: Glastech.Ber. *61*, 59 (1988).
22. Claußen O., Rüssel C.: Glastech.Ber. *69*, 95 (1996).
23. De Strycker J., Westbroek P., Temmerman E.: Electrochem.Commun. *4*, 41 (2002).

ZKOUMÁNÍ MECHANISMŮ OXIDACE MOLYBDENU VE SKLOVINĚ

INE VANMOORTEL, JOOST DE STRYCKER*,
EDUARD TEMMERMAN, ANNEMIE ADRIAENS

Department of Analytical Chemistry, Ghent University,
Krijgslaan 281-S12, B-9000 Ghent, Belgium
**Arcelor Innovation - R&D, OCAS N.V.,*
J. Kennedylaan 3, B-9060 Zelzate, Belgium

Tato studie se zaměřuje na vypracování mechanismů oxidace molybdenu ve sklovině. Konkrétně bylo snahou zjistit, zda k anodickému rozpouštění molybdenu dochází v jednom nebo ve více krocích, a jaké jsou produkty reakce. Studie byla provedena ve dvou stupních. Nejprve byly zkoumány reakce iontů molybdenu ve sklovině na platinové elektrodě. Následovalo zkoumání korozních reakcí ve sklovině na molybdenové elektrodě. Experimenty ukázaly, že k oxidaci molybdenu dochází ve třech krocích: Mo → Mo^{3+}(sklo) + 3e^- (I); Mo^{3+}(sklo) → Mo^{4+}(povrch/sklo) + e^- nebo Mo → Mo^{4+}(povrch/sklo) + 4e^- (II); Mo^{4+} (povrch/sklo) → Mo^{6+}(sklo) + 2e^- nebo Mo → Mo^{6+}(sklo) + 6e^- (III).